BASIC CONCEPTS OF TIME-RESOLVED MOLECULAR SPECTROSCOPY

Jeffrey A. Cina
University of Oregon

July 1, 2011

For Barbara, of course.

Contents

1 Phase-coherent multidimensional electronic spectroscopy signals from an energy-transfer complex — wave-packet pictures for two measurement strategies and three electronic bases

1.1 Molecular Hamiltonian for an energy-transfer dimer

In this chapter we work through the basic description of phase-coherent multidimensional electronic spectroscopy measurements on a molecular dimer comprising four electronic *site states*, $|gg\rangle$, $|eg\rangle$, $|ge\rangle$, and $|ee\rangle$, in which neither, either one, or both of the monomers is electronically excited.[1] The dimer Hamiltonian is $H = T + H_{el}(\hat{Q})$,[2] where T is the nuclear kinetic energy. The electronic Hamiltonian in the site representation is given by

$$\begin{aligned} H_{el}(Q) &= |gg\rangle\, V_{gg}(Q)\, \langle gg| + |ge\rangle\, V_{ge}(Q)\, \langle ge| + |eg\rangle\, V_{eg}(Q)\, \langle eg| \\ &\quad + |ee\rangle\, V_{ee}(Q)\, \langle ee| + J(Q)\, (|eg\rangle\langle ge| + |ge\rangle\langle eg|)\,. \end{aligned} \tag{1.1.1}$$

Q stands for the full collection of intramolecular and intermolecular nuclear coordinates, including those of any surrounding medium. Alternatively, in the basis of *adiabatic electronic states*,

$$\begin{aligned} H_{el}(Q) &= |0\rangle\, E_0(Q)\, \langle 0| + \left|1'(Q)\right\rangle V_{1'}(Q)\, \left\langle 1'(Q)\right| \\ &\quad + |1(Q)\rangle\, V_1(Q)\, \langle 1(Q)| + |2\rangle\, V_2(Q)\, \langle 2|\,. \end{aligned} \tag{1.1.2}$$

The relationship between these two representations of the electronic Hamiltonian is easy to determine. Let

$$\mathcal{P}_{one} = |eg\rangle\langle eg| + |ge\rangle\langle ge|\,, \tag{1.1.3}$$

$$\sigma_x = |eg\rangle\langle ge| + |ge\rangle\langle eg|\,, \tag{1.1.4}$$

$$\sigma_y = -i\,|eg\rangle\langle ge| + i\,|ge\rangle\langle eg|\,, \tag{1.1.5}$$

and

$$\sigma_z = |eg\rangle\langle eg| - |ge\rangle\langle ge|\,. \tag{1.1.6}$$

[1] We neglect states involving higher electronic excitation of either monomer, such as $|e'g\rangle$ or $|e'e''\rangle$.

[2] We use hats when it may be specifically helpful to identify quantum mechanical operators.

Figure 1.1.1: Parameters of electronic Hamiltonian. $J(Q)$ specifies the energy-transfer coupling at nuclear configuration Q. $K(Q)$ is half the local site-energy difference. $M(Q)$ is half the resultant energy difference between adiabatic singly-excited electronic states.

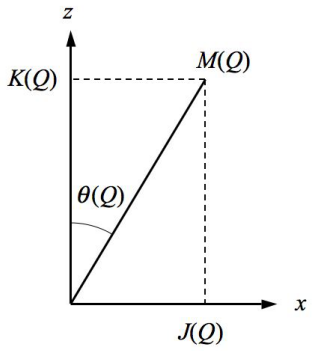

Then Eq. (1.1.1) becomes

$$\begin{aligned} H_{el}(Q) &= |gg\rangle\langle gg|\, V_{gg}(Q) + \mathcal{P}_{one} L(Q) + \sigma_z M(Q)\cos\theta(Q) \\ &\quad + \sigma_x M(Q)\sin\theta(Q) + |ee\rangle\langle ee|\, V_{ee}(Q) \\ &= |gg\rangle\langle gg|\, V_{gg}(Q) + \mathcal{P}_{one} L(Q) \\ &\quad + e^{-i\sigma_y\theta(Q)/2}\sigma_z e^{i\sigma_y\theta(Q)/2} M(Q) + |ee\rangle\langle ee|\, V_{ee}(Q). \end{aligned} \tag{1.1.7}$$

We have introduced the following functions of the nuclear coordinates:

$$K(Q) = \frac{1}{2}\left(V_{eg}(Q) - V_{ge}(Q)\right), \tag{1.1.8}$$

$$L(Q) = \frac{1}{2}\left(V_{eg}(Q) + V_{ge}(Q)\right), \tag{1.1.9}$$

and

$$M(Q) = \sqrt{J^2(Q) + K^2(Q)}. \tag{1.1.10}$$

The angle $\theta(Q) = \arctan\left[J(Q)/K(Q)\right]$ is illustrated in Figure 1.1.1.

Exercise: Use the properties of the Pauli operators (1.1.4), (1.1.5), and (1.1.6) to obtain expression (1.1.7) for the electronic Hamiltonian.

The adiabatic eigenenergies appearing in Eq. (1.1.2) can be seen from (1.1.7) to be

$$E_0(Q) = V_{gg}(Q), \tag{1.1.11}$$

$$E_{1'}(Q) = L(Q) - M(Q), \tag{1.1.12}$$

$$E_1(Q) = L(Q) + M(Q), \tag{1.1.13}$$

and

$$E_2(Q) = V_{ee}(Q), \tag{1.1.14}$$

while the corresponding adiabatic electronic eigenstates are

$$|0\rangle = |gg\rangle\,, \tag{1.1.15}$$

$$\left|1'(Q)\right\rangle = \exp\left\{-i\frac{\theta(Q)}{2}\sigma_y\right\}|ge\rangle\,, \tag{1.1.16}$$

$$|1(Q)\rangle = \exp\left\{-i\frac{\theta(Q)}{2}\sigma_y\right\}|eg\rangle\,, \tag{1.1.17}$$

and

$$|2\rangle = |ee\rangle\,. \tag{1.1.18}$$

Yet another electronic basis is also popular. We identify the adiabatic electronic states at the fixed nuclear configuration corresponding to the equilibrium position $Q = 0$ of the electronic ground state as the *exciton basis*,

$$|0\rangle = |gg\rangle\,, \tag{1.1.19}$$

$$\left|1'\right\rangle = \left|1'(0)\right\rangle = |ge\rangle\cos\frac{\theta}{2} - |eg\rangle\sin\frac{\theta}{2}, \tag{1.1.20}$$

$$|1\rangle = |1(0)\rangle = |ge\rangle\sin\frac{\theta}{2} + |eg\rangle\cos\frac{\theta}{2}, \tag{1.1.21}$$

and

$$|2\rangle = |ee\rangle\,. \tag{1.1.22}$$

In terms of these we can write $H_{el}(Q) = H_{el} + \upsilon(Q)$, with

$$H_{el} = H_{el}(0) = |0\rangle\,E_0\,\langle 0| + \left|1'\right\rangle E_{1'}\left\langle 1'\right| + |1\rangle\,E_1\,\langle 1| + |2\rangle\,E_2\,\langle 2| \tag{1.1.23}$$

and, from Eq. (1.1.1),

$$\begin{aligned}\upsilon(Q) &= H_{el}(Q) - H_{el} \\ &= |gg\rangle\,\delta V_{gg}(Q)\,\langle gg| + |ge\rangle\,\delta V_{ge}(Q)\,\langle ge| + |eg\rangle\,\delta V_{eg}(Q)\,\langle eg| \\ &\quad + |ee\rangle\,\delta V_{ee}(Q)\,\langle ee| + (|eg\rangle\langle ge| + |ge\rangle\langle eg|)\,\delta J(Q),\end{aligned} \tag{1.1.24}$$

in which $\delta V_{gg}(Q) = V_{gg}(Q) - V_{gg}$ and so forth.

Figure 1.1.2: Left panel shows contour plot of $V_{ge}(Q_a, Q_b)$ for downhill EET dimer; minimum value is ϵ_{ge} at $(Q_a, Q_b) = (0, 2d_a)$. Right panel is $V_{eg}(Q_a, Q_b)$, with minimum value $\epsilon_{ge} + M\omega_a^2 d_a^2$ at $(Q_a, Q_b) = (d_a, 0)$. Dashed diagonal in both panels is the line of intersection between the two potential surfaces.

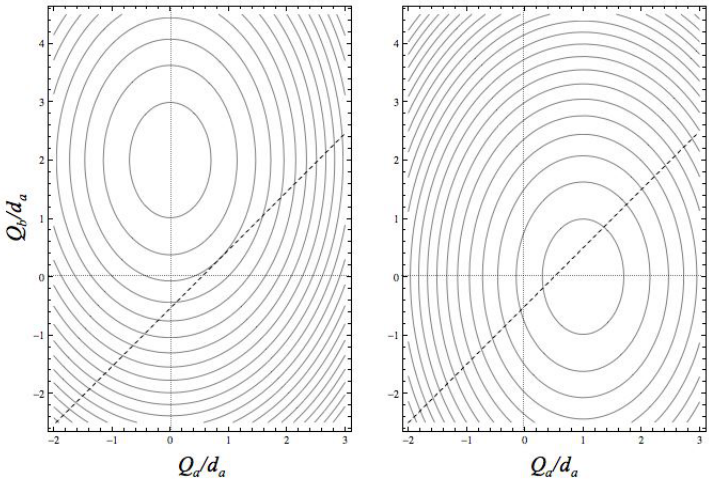

To make these concepts concrete, we consider a model electronic Hamiltonian of the form (1.1.1) with site-state potentials

$$V_{gg}(Q_a, Q_b) = \frac{M\omega_a^2}{2} Q_a^2 + \frac{M\omega_b^2}{2} Q_b^2 \,, \tag{1.1.25}$$

$$V_{ge}(Q_a, Q_b) = \frac{M\omega_a^2}{2} Q_a^2 + \frac{M\omega_b^2}{2} (Q_b - d_b)^2 + \epsilon_{ge} \,, \tag{1.1.26}$$

$$V_{eg}(Q_a, Q_b) = \frac{M\omega_a^2}{2} (Q_a - d_a)^2 + \frac{M\omega_b^2}{2} Q_b^2 + \epsilon_{eg} \,, \tag{1.1.27}$$

and

$$V_{ee}(Q_a, Q_b) = \frac{M\omega_a^2}{2} (Q_a - d_a)^2 + \frac{M\omega_b^2}{2} (Q_b - d_b)^2 + \epsilon_{ee} \,. \tag{1.1.28}$$

We make the specific choices $\omega_b = \omega_a/\sqrt{2}$, $d_b = 2d_a$, $\epsilon_{eg} = \epsilon_{ge} + M\omega_a^2 d_a^2$, and $J = M\omega_a^2 d_a^2/10$, so the monomers are weakly coupled and the dimer exhibits "downhill" energy transfer from state-*eg* to state-*ge*. Figure (1.1.2) shows contour plots of the singly-excited site energies (1.1.26) and (1.1.27) of the "acceptor-excited" and "donor-excited" states, respectively.

The adiabatic potential-energy surfaces $E_{1'}(Q_a, Q_b)$ and $E_1(Q_a, Q_b)$ for this model Hamiltonian, given by Eqs. (1.1.12) and (1.1.13), respectively, are plotted in Figure (1.1.3). The gray dot at the origin in each plot identifes the corresponding exciton energy, $E_{1'}$ or E_1.

Figure 1.1.3: Left panel shows the lower-lying singly-excited adiabatic potential-energy surface $E_{1'}(Q_a, Q_b)$. Its minima near $(Q_a, Q_b) = (0, 2d_a)$ and $(d_a, 0)$ have values similar to those of $V_{ge}(Q_a, Q_b)$ and $V_{eg}(Q_a, Q_b)$, respectively. Right panel gives the higer-lying $E_1(Q_a, Q_b)$, whose minumum value is $2.24(M\omega_a^2 d_a^2/2) + \epsilon_{ge}$ at $(0.787d_a, 0.427d_a)$. Note that energy spacing between contours is about twice as large in the right panel as in the left.

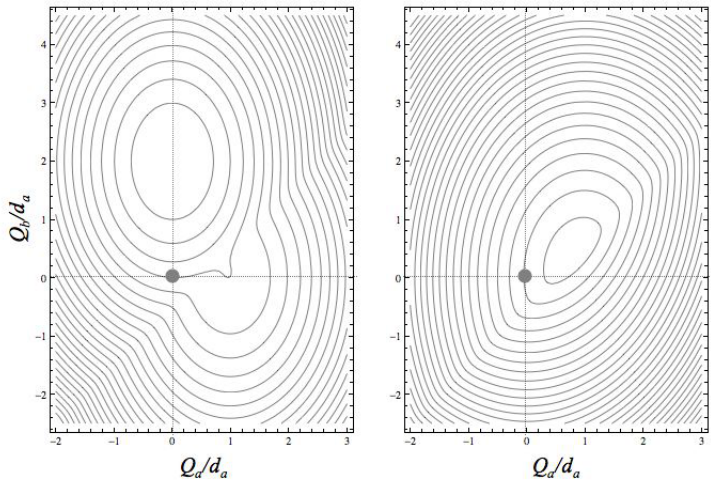

Exercise: Show that the Q-dependent part (1.1.24) of the electronic Hamiltonian is given in the exciton representation by

$$\begin{aligned} \upsilon(Q) &= |0\rangle\langle 0|\,\delta V_{gg}(Q) + \left|1'\right\rangle\left\langle 1'\right|\left[\delta L(Q) - \delta K(Q)\cos\theta - \delta J(Q)\sin\theta\right] \\ &\quad + |1\rangle\langle 1|\left[\delta L(Q) + \delta K(Q)\cos\theta + \delta J(Q)\sin\theta\right] \\ &\quad + \left(|1\rangle\left\langle 1'\right| + \left|1'\right\rangle\langle 1|\right)\left[-\delta K(Q)\sin\theta + \delta J(Q)\cos\theta\right] \\ &\quad + |2\rangle\langle 2|\,\delta V_{ee}(Q). \end{aligned} \tag{1.1.29}$$

1.2 Pulse sequence and time-dependent molecular state

In order to compare four-wave-mixing (FWM) and fluorescence-detected wave-packet-interferometry (WPI) approaches to multidimensional electronic spectroscopy measurements on electronic-excitation-transfer (EET) systems, we add a time-dependent field-interaction term $V(t) = -\hat{\mathbf{m}}\cdot\mathbf{E}(t)$ to the Hamiltonian. The dipole moment operator is given in the site representation by

$$\hat{\mathbf{m}} = \mathbf{m}_a\left(|eg\rangle\langle gg| + |ee\rangle\langle ge|\right) + \mathbf{m}_b\left(|ge\rangle\langle gg| + |ee\rangle\langle eg|\right) + H.c. \tag{1.2.1}$$

It is a straightforward exercise to obtain from (1.2.1) an expression for the dimer's dipole moment operator in the adiabatic representation, and from the latter to find the dipole operator in the exciton representation,

$$\begin{aligned} \hat{\mathbf{m}} &= \left|1'\right\rangle\langle 0|\left(-\mathbf{m}_a\sin\frac{\theta}{2} + \mathbf{m}_b\cos\frac{\theta}{2},\right) + |1\rangle\langle 0|\left(\mathbf{m}_a\cos\frac{\theta}{2} + \mathbf{m}_b\sin\frac{\theta}{2}\right) \\ &\quad + |2\rangle\left\langle 1'\right|\left(\mathbf{m}_a\cos\frac{\theta}{2} - \mathbf{m}_b\sin\frac{\theta}{2}\right) + |2\rangle\langle 1|\left(\mathbf{m}_a\sin\frac{\theta}{2} + \mathbf{m}_b\cos\frac{\theta}{2}\right) \\ &\quad + H.c., \end{aligned} \tag{1.2.2}$$

by setting $Q = 0$.

Exercise: Do this.

The electric field consists of four ultrashort light pulses:

$$\mathbf{E}(t) = \sum_{I=A,B,C,D} \mathbf{E}_I(t); \tag{1.2.3}$$

$$\mathbf{E}_I(t) = \mathbf{e}_I E_I f_I\left(t - t_I(\mathbf{r})\right) \cos\Phi\left(t - t_I(\mathbf{r})\right). \tag{1.2.4}$$

Here, $\mathbf{e}_I$ is a real unit vector specifying the laser polarization. $f_I(t)$ is an envelope function localized around $t = 0$ and having a temporal width $\sim \sigma_I$. The phase function has the form $\Phi_I(t) = \Omega_I t + \varphi_I$, and the arrival time $t_I(\mathbf{r}) = t_I + \mathbf{n}_I \cdot \mathbf{r}/c$ depends on the location of the complex—assumed fixed within the sample; $\mathbf{n}_I$ is a unit vector in the direction of of propagation of the I^{th} laser pulse, and c is the speed of light. The pulses arrive in sequence; we will typically assume $t_A \leqq t_B \leqq t_C \leqq t_D$ (but when we consider FWM signals monitored by spectral interferometry, will instead take $t_D << t_A \leqq t_B \leqq t_C$). We specialize to the common experimental situation of two phase-controlled pulse-pairs in which the optical phase *differences* $\varphi_{BA} = \varphi_B - \varphi_A$ and $\varphi_{DC} = \varphi_D - \varphi_C$ are specified, but the individual absolute phases φ_I vary randomly on successive laser shots as a result of mechanical jitter on the scale of an optical wave-length.

The evolution of the dimer's state-ket in the presence of the perturbation $V(t) = -\hat{\mathbf{m}} \cdot \mathbf{E}(t)$ is specified by the time-dependent Schrödinger equation,

$$i\hbar \frac{\partial}{\partial t} \left|\Psi(t)\right\rangle = \left(H + V(t)\right) \left|\Psi(t)\right\rangle, \tag{1.2.5}$$

with the initial condition,

$$\left|\Psi\left(t << t_A(\mathbf{r})\right)\right\rangle = \exp\{-iH\left(t - t_A(\mathbf{r})\right)/\hbar\} \left|gg\right\rangle \left|\psi_\circ\right\rangle, \tag{1.2.6}$$

where $|\psi_\circ\rangle$ can be an eigenstate of the nuclear Hamlitonian $T + \langle gg| H_{el}(\hat{Q}) |gg\rangle = T + E_0(\hat{Q})$ associated with the electronic ground state or a nuclear wave packet—an arbitrary linear superposition of such eigenstates. We seek a perturative solution to Eq. (1.2.5) by switching to the interaction picture

$$\left|\tilde{\Psi}(t)\right\rangle = \exp\{iH\left(t - t_A(\mathbf{r})\right)/\hbar\} \left|\Psi(t)\right\rangle, \tag{1.2.7}$$

with the initial condition $\left|\tilde{\Psi}(t << t_A(\mathbf{r}))\right\rangle = |gg\rangle|\psi_\circ\rangle$. The Schrödinger equation in the interaction picture becomes

$$i\hbar \frac{\partial}{\partial t} \left|\tilde{\Psi}(t)\right\rangle = \tilde{V}(t) \left|\tilde{\Psi}(t)\right\rangle, \tag{1.2.8}$$

with $\tilde{V}(t) = \exp\{iH\left(t - t_A(\mathbf{r})\right)/\hbar\} V(t) \exp\{-iH\left(t - t_A(\mathbf{r})\right)/\hbar\}$. After adopting the streamlined notation $[t] = \exp\{-iHt/\hbar\}$, introducing *pulse propagators* defined by

$$P_I(t;\tau) = \frac{i}{\hbar} \int_{-\infty}^{t} d\tau \left[t_I(\mathbf{r}) - \tau\right] \hat{\mathbf{m}} \cdot \mathbf{E}_I(\tau) [\tau - t_I(\mathbf{r})], \tag{1.2.9}$$

and returning to the Schrödinger picture, the perturbative solution through third order in the laser fields is found to be

$$
\begin{aligned}
|\Psi(t)\rangle \;=\; & [t - t_A(\mathbf{r})] \Bigg\{ 1 + \sum_{I=A,B,C,D} [t_{AI}(\mathbf{r})] P_I(t;\tau) [t_{IA}(\mathbf{r})] \\
& + \sum_{IJ} [t_{AI}(\mathbf{r})] P_I(t;\tau) [t_{IJ}(\mathbf{r})] P_J(\tau;\bar{\tau}) [t_{JA}(\mathbf{r})] \\
& + \sum_{IJK} [t_{AI}(\mathbf{r})] P_I(t;\tau) [t_{IJ}(\mathbf{r})] P_J(\tau;\bar{\tau}) [t_{JK}(\mathbf{r})] \\
& \times P_K(\bar{\tau};\bar{\bar{\tau}}) [t_{KA}(\mathbf{r})] \Bigg\} |gg\rangle \, |\psi_\circ\rangle \,, \qquad (1.2.10)
\end{aligned}
$$

in which $t_{IJ} = t_I - t_J$.[3,4,5]

Exercise: Verify the solution (1.2.10). Explain why the state-ket through third order in the perturbation is sufficient for calculating the expectation value of an observable that is quadrilinear in the laser electric fields (i.e., proportional to $E_A E_B E_C E_D$).

1.3 Pulse propagators

We could work out expressions for the FWM and fluorescence-detected WPI signals using any of the three electronic bases, but bypass the adiabatic basis in favor of the two fixed bases $\{|gg\rangle\,, |ge\rangle\,, |eg\rangle\,, |ee\rangle\}$ and $\{|0\rangle\,, |1'\rangle\,, |1\rangle\,, |2\rangle\}$, and use a common symbol $|\xi\rangle$ to refer to a member of either the site or the exciton basis. For the sake of the simplification thereby enabled, we'll assume that the pulses impinging on the sample are genuinely ultrafast on at least one relevant timescale. Either $\sigma << |2\pi/J|$, so that EET can be neglected for the duration of a laser pulse, or $\sigma << |2\pi/\upsilon|$, so the pulses "freeze" nuclear motion (or both). The former (latter) condition is the easier one to satisfy if the energy-transfer coupling is smaller (larger) than the Franck-Condon energies. In the first

[3] Because the square-bracket notation for time-evolution operators is used only with a single time argument, there should be no cause for confusion with commutators or with the use of square brackets as a grouping device for quantities having dimensions other than time.

[4] The difference in position-dependent arrival times becomes $t_{IJ}(\mathbf{r}) = t_I(\mathbf{r}) - t_J(\mathbf{r}) = t_{IJ} + \mathbf{n}_{IJ} \cdot \mathbf{r}/c$, where $\mathbf{n}_{IJ} = \mathbf{n}_I - \mathbf{n}_J$ need not be a unit vector.

[5] The expansion (1.2.10) may involve some nested integrals. In the double sum, for instance, the integration variable τ in $P_I(t;\tau)$ is the upper integration limit of $P_J(\tau;\bar{\tau})$. But the resulting double integration reduces to a product of single integrals unless pulses I and J are temporally overlapping.

instance, it is convenient to work in the site basis; in the second, it is natural to use the exciton basis.

In the appropriate basis (or bases), the matrix elements of the pulse propagators (1.2.9) can be determined with the aid of the rotating wave approximation:

$$\langle \xi | \, P_I(t;\tau) \, | \bar{\xi} \rangle = i E_I (\xi\bar{\xi})_I e^{\mp i\varphi_I} p_I^{(\xi\bar{\xi})}(t;\tau). \tag{1.3.1}$$

In this equation, we denote the projection of an electronic transition dipole moment on a laser-polarization vector by $(\xi\bar{\xi})_I = \mathbf{m}_{\xi\bar{\xi}} \cdot \mathbf{e}_I$. For an upward (or downward) electronic transition $\xi \leftarrow \bar{\xi}$ (or $\bar{\xi} \rightarrow \xi$), we use the upper (or lower) sign in the exponent of Eq. (1.3.1) involving the optical phase φ_I. This formula also introduces a nuclear operator, the *reduced pulse propagator*,

$$p_I^{(\xi\bar{\xi})}(t;\tau) = \frac{1}{2\hbar} \int_{-\infty}^{t} d\tau \; [t_I(\mathbf{r}) - \tau]_{\xi\xi} \, [\tau - t_I(\mathbf{r})]_{\bar{\xi}\bar{\xi}} \, f_I \left(\tau - t_I(\mathbf{r})\right) e^{\mp i \Omega_I (\tau - t_I(\mathbf{r}))}, \tag{1.3.2}$$

in which the single-state evolution operators $[t]_{\xi\xi} = \langle \xi | \, [t] \, | \xi \rangle$ and $[t]_{\bar{\xi}\bar{\xi}}$ are to be calculated with J (or v) set equal to zero if $|\xi\rangle$ is a site (or exciton) state. The definition (1.3.2) employs the same sign convention as (1.3.1) in the exponent involving the carrier frequency Ω_I. When applied to a nuclear wave packet in the $\bar{\xi}$ electronic state, $p_I^{(\xi\bar{\xi})}$ describes its distortion, if any, upon transition to state ξ under the influence of pulse I.

Exercises:

- Check the expression (1.3.1) for matrix elements of the pulse propagator of an electronically resonant laser pulse, paying particular attention to the neglect, under the rotating-wave approximation, of the ineffectual, counter-rotating term in the integrand.
- Make use of the anti-Hermitian property $P_I^\dagger(t;\tau) = -P_I(t;\tau)$ of the pulse propagators (1.2.9) to show that the reduced pulse propagators obey $\left(p_I^{(\xi\bar{\xi})}(t;\tau)\right)^\dagger = p_I^{(\bar{\xi}\xi)}(t;\tau)$.
- Under what condition would $p_I^{(\xi\bar{\xi})}$ *not* distort the nuclear wave packet it transfers from state $\bar{\xi}$ to state ξ?

1.4 Trilinear dipole moment and quadrilinear excited-state populations

We will consider two general strategies for measuring a two-dimensional electronic spectroscopy signal and use the third-order expansion (1.2.10) for $|\Psi(t)\rangle$ to calculate the

Figure 1.4.1: Arrangement of the chromophore-dimer location $\mathbf{r}$ within sample volume and the field point $\mathbf{R}$.

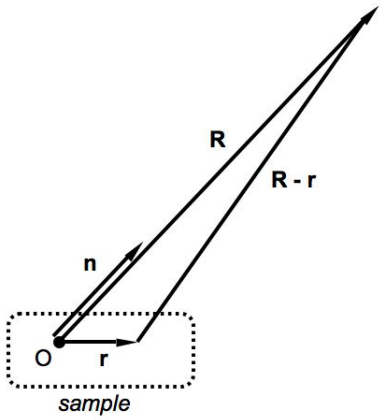

requisite expectation values in each case. In the FWM approach, one observes a signal electric field at field point $\mathbf{R} = R\mathbf{n}$ that is distant from the sample (Figure 1.4.1). The signal field of interest is generated by the combined action of the *trilinear dipole moments*[6] $\mathbf{m}_{ABC}(t)$ of all illuminated chromophores. In an alternative, multidimensional WPI experiment, one observes fluorescence—or some other population-sensitive action signal—to determine the quantum-yield-weighted sum of the quadrilinear contribution to the population (proportional to $E_A E_B E_C E_D$) in the various electronic excited states.

To calculate the trilinear radiated field at field point $\mathbf{R}$ at time t, we need the molecular state at the earlier time $t - |\mathbf{R} - \mathbf{r}|/c \cong t - (R - \mathbf{r} \cdot \mathbf{n})/c$. To evaluate the quadrilinear excited-state populations contributing to the WPI signal, on the other hand, we may use the state $|\Psi(t)\rangle$ with its time argument formally set equal to the arrival time of the fourth pulse, $t_D(\mathbf{r}) = t_D + \mathbf{n}_D \cdot \mathbf{r}/c$. Thus the relevant time arguments of the free-evolution operators $[t]$ appearing in (1.2.10) are of two possible forms,

$$t - \frac{|\mathbf{R} - \mathbf{r}|}{c} - t_A(\mathbf{r}) \cong t - \frac{R}{c} + \frac{\mathbf{r} \cdot (\mathbf{n} - \mathbf{n}_A)}{c}; \text{ (FWM only)}, \tag{1.4.1}$$

or

$$t_{IJ}(\mathbf{r}) = t_{IJ} + \frac{\mathbf{n}_{IJ} \cdot \mathbf{r}}{c} \text{ (FWM and WPI)}. \tag{1.4.2}$$

To prevent degradation of the experimental time resolution by "geometrical broadening" of the interpulse delays, the angle θ_{IJ} between propagation directions must be small enough that $|\mathbf{n}_{IJ} \cdot \mathbf{r}|/c \approx a\theta_{IJ}/c << \sigma$, where a is diameter of a laser spot.[7] This

[6] By which is meant the portion of the time-dependent dipole moment expectation value proportional to $E_A E_B E_C$.

[7] FWM signal beams will be seen shortly to emerge in the directions $\mathbf{n}_A - \mathbf{n}_B + \mathbf{n}_C$ and $\mathbf{n}_B - \mathbf{n}_A + \mathbf{n}_C$; nonnegligible signal field can only be observed at points $\mathbf{R} = R\mathbf{n}$ for which $\mathbf{n}$ closely approximates

criterion—that the divergence of the beams across the sample be less than the distance light travels in time σ—implies

$$\frac{a}{c}\theta_{IJ} << \sigma << \begin{cases} \left|2\pi/J\right|, & \text{when pulses freeze EET} \\ \left|2\pi/v\right|, & \text{when pulses freeze vibrations} \end{cases}. \tag{1.4.3}$$

It is therefore reasonable to suppose the interbeam angles are small enough that $a\theta_{IJ}/c$ is negligible on the timescales of *both* EET and nuclear motion, regardless of which one is shorter.

Geometrical broadening may not be negligible on the remaining, *optical* timescale $\sim 2\pi/\Omega$, the period of light resonant with an electronic transition. We can take advantage of the fact that only energy transfer and electron-vibration coupling, which are negligible on the timescale of $\mathbf{n}_{IJ}\cdot\mathbf{r}/c$, can induce electronic transitions and approximate the matrix elements of a time-evolution operator as

$$\begin{aligned} \left[t_{IJ} + \frac{\mathbf{n}_{IJ}\cdot\mathbf{r}}{c}\right]_{\xi\bar{\xi}} &= \sum_{\xi'} \left[t_{IJ}\right]_{\xi\xi'} \left[\frac{\mathbf{n}_{IJ}\cdot\mathbf{r}}{c}\right]_{\xi'\bar{\xi}} \\ &\cong \left[t_{IJ}\right]_{\xi\bar{\xi}} \left[\frac{\mathbf{n}_{IJ}\cdot\mathbf{r}}{c}\right]_{\bar{\xi}\bar{\xi}} \\ &\cong \left[t_{IJ}\right]_{\xi\bar{\xi}} \exp\left\{-i\eta_{\bar{\xi}}(\mathbf{k}_I - \mathbf{k}_J)\cdot\mathbf{r}\right\}, \end{aligned} \tag{1.4.4}$$

where the *excitation number* of state $\bar{\xi}$, specified by

$$\eta_{\bar{\xi}} = \begin{cases} 0 & \bar{\xi} = 0\,(gg) \\ 1 & \bar{\xi} = 1', 1\,(ge, eg) \\ 2 & \bar{\xi} = 2\,(ee) \end{cases}, \tag{1.4.5}$$

and the *wave vector* $\mathbf{k}_I = \Omega_I \mathbf{n}_I/c$ of beam I have been introduced.

To find expressions for the trilinear dipole moment and the quadrilinear excited-state populations, we need not calculate all the terms in the expansion (1.2.10)—which, for instance, includes terms in which a single field strength appears at second or third order—but must only determine the specific multilinear nuclear amplitudes in each of the four electronic states that can contribute to the expectation values of interest. For our purposes then, the relevant amplitude in the doubly-excited electronic state comprises only the four bilinear terms:

$$\begin{aligned} \langle ee\,|\Psi(t)\rangle &= \langle 2\,|\Psi(t)\rangle \\ &= \langle 2\,|\Psi_{AC}(t)\rangle + \langle 2\,|\Psi_{BC}(t)\rangle + \underbrace{\langle 2\,|\Psi_{AD}(t)\rangle + \langle 2\,|\Psi_{BD}(t)\rangle}_{\text{nonexistent in FWM}}. \end{aligned} \tag{1.4.6}$$

Subscripts identify the participating pulses in each contributing nuclear wave packet. AB and CD terms in $\langle ee\,|\Psi(t)\rangle$ are omitted as they cannot play any role in the measured

one of these two directions. The conditions forestalling geometrical broadening are therefore the same in FWM and md-WPI experiments.

FWM or md-WPI signals: they carry uncontrolled optical phase factors $\exp\{-i\varphi_A - i\varphi_B\}$ and $\exp\{-i\varphi_C - i\varphi_D\}$, respectively, which cause any expectation value in which they appear to average to zero over many laser shots (see page 13). In a FWM measurement, the signal field radiated by the trilinear dipole moments within the illuminated volume interfere with the *local oscillator* (D-pulse) in the far-field region (see Figure 1.4.1); it is not even necessary for the local-oscillator beam to pass through the sample, and, as indicated in Eq. (1.4.6), the two-pulse amplitudes involving the D-pulse do not enter the FWM signal expression.

There are both one-pulse and three-pulse contributions to the nuclear amplitudes accompanying the one-exciton $\xi = ge, eg$ (or $1', 1$) states:

$$\begin{aligned} \langle \xi \,|\Psi(t)\rangle \;\; = \;\; & \langle \xi \,|\Psi_A(t)\rangle + \langle \xi \,|\Psi_B(t)\rangle + \langle \xi \,|\Psi_C(t)\rangle + \langle \xi \,|\Psi_{ABC}(t)\rangle \\ & + \underbrace{\langle \xi \,|\Psi_D(t)\rangle + \langle \xi \,|\Psi_{ABD}(t)\rangle + \langle \xi \,|\Psi_{ACD}(t)\rangle + \langle \xi \,|\Psi_{BCD}(t)\rangle}_{\text{nonexistent in FWM}}. \end{aligned} \tag{1.4.7}$$

The nuclear amplitude in the electronic ground state has zero- and two-pulse terms:

$$\begin{aligned} \langle gg \,|\Psi(t)\rangle \;\; = \;\; & \langle 0 \,|\Psi(t)\rangle \\ & + [t - t_A]_{00} \,|\psi_\circ\rangle + \langle 0 \,|\Psi_{AB}(t)\rangle + \langle 0 \,|\Psi_{AC}(t)\rangle + \langle 0 \,|\Psi_{BC}(t)\rangle \\ & + \underbrace{\langle 0 \,|\Psi_{AD}(t)\rangle + \langle 0 \,|\Psi_{BD}(t)\rangle + \langle 0 \,|\Psi_{CD}(t)\rangle}_{\text{nonexistent in FWM}}. \end{aligned} \tag{1.4.8}$$

Again in Eqs. (1.4.7) and (1.4.8), the terms involving the D-pulse do not contribute to the FWM signal.

The trilinear dipole moment can be determined by using the dimer state-ket in the form

$$|\Psi(t)\rangle = |gg\rangle \langle gg|\, \Psi(t)\rangle + |ge\rangle \langle ge|\, \Psi(t)\rangle + |eg\rangle \langle eg|\, \Psi(t)\rangle + |ee\rangle \langle ee|\, \Psi(t)\rangle \tag{1.4.9}$$

(or the analogous expression in the exciton representation) and, with the help of Eqs. (1.4.6) through (1.4.8), isolating the portion of the expectation value $\langle \Psi(t)|\, \hat{\mathbf{m}}\, |\Psi(t)\rangle$ that is simultaneously linear in the A-, B-, and C-pulse field strength parameters. The result of this procedure is

$$\begin{aligned} \mathbf{m}_{ABC}(t) \;\; = \;\; & 2\mathrm{Re} \sum_\xi \{ \langle \psi_\circ |\, [-t + t_A(\mathbf{r})]_{00} \mathbf{m}_{0\xi} \langle \xi \,|\Psi_{ABC}(t)\rangle \\ & + \langle \Psi_{BC}(t) \,|0\rangle \, \mathbf{m}_{0\xi} \langle \xi \,|\Psi_A(t)\rangle + \langle \Psi_B(t) \,|\xi\rangle \, \mathbf{m}_{\xi 0} \langle 0 \,|\Psi_{AC}(t)\rangle \\ & + \langle \Psi_C(t) \,|\xi\rangle \, \mathbf{m}_{\xi 0} \langle 0 \,|\Psi_{AB}(t)\rangle + \langle \Psi_{BC}(t) \,|2\rangle \, \mathbf{m}_{2\xi} \langle \xi \,|\Psi_A(t)\rangle \\ & + \langle \Psi_B(t) \,|\xi\rangle \, \mathbf{m}_{\xi 2} \langle 2 \,|\Psi_{AC}(t)\rangle \}; \end{aligned} \tag{1.4.10}$$

the sum is over $\xi = 1', 1$ or ge, eg, depending on the choice of basis.

The portions of the excited-state populations that are simultaneously linear in A-, B-, C-, and D-pulse electric field strengths are found to be

$$\begin{aligned} S^{(ee)}(t) \;\; &= \;\; S^{(2)}(t) \\ &= \;\; 2\mathrm{Re} \{ \langle \Psi_{BC}(t) \,|2\rangle\langle 2 \,|\Psi_{AD}(t)\rangle + \langle \Psi_{BD}(t) \,|2\rangle\langle 2 \,|\Psi_{AC}(t)\rangle \} \end{aligned} \tag{1.4.11}$$

and, for $\xi = ge, eg$ or $1', 1$,

$$\begin{aligned} S^{(\xi)}(t) &= 2\mathrm{Re}\left\{\langle\Psi_D(t)|\xi\rangle\langle\xi|\Psi_{ABC}(t)\rangle + \langle\Psi_C(t)|\xi\rangle\langle\xi|\Psi_{ABD}(t)\rangle\right. \\ &\quad \left. + \langle\Psi_B(t)|\xi\rangle\langle\xi|\Psi_{ACD}(t)\rangle + \langle\Psi_{BCD}(t)|\xi\rangle\langle\xi|\Psi_A(t)\rangle\right\}. \end{aligned} \tag{1.4.12}$$

1.5 Four-wave-mixing signal

The stage is now set to find the basic expression for the FWM signal and (in the next section) the md-WPI signal. The electric field generated in the far field by the oscillating dipole moments $\mathbf{m}_{ABC}(t)$ of all the laser-illuminated chromophore pairs is

$$\begin{aligned} \mathbf{E}_{ABC}(t) &= \frac{1}{c^2 R}\sum_{\mathbf{r}}\left[\ddot{\mathbf{m}}_{ABC}\left(t - \frac{R}{c} + \frac{\mathbf{n}\cdot\mathbf{r}}{c}\right)\times\mathbf{n}\right]\times\mathbf{n} \\ &= -\frac{1}{c^2 R}\sum_{\mathbf{r}}(1-\mathbf{nn})\cdot\ddot{\mathbf{m}}_{ABC}\left(t - \frac{R}{c} + \frac{\mathbf{n}\cdot\mathbf{r}}{c}\right), \end{aligned} \tag{1.5.1}$$

where the sum is over dimer locations.[8] If we define ρ as the average number density of dimers within the sample volume V, and take advantage of the relatively narrow range of electronic excitation frequencies to write $\ddot{\mathbf{m}} \approx -\Omega^2\mathbf{m}$, then

$$\mathbf{E}_{ABC}(t) \cong \frac{\rho\Omega^2}{c^2 R}(1-\mathbf{nn})\cdot\int_V d^3r\,\mathbf{m}_{ABC}\left(t - \frac{R}{c} + \frac{\mathbf{n}\cdot\mathbf{r}}{c}\right). \tag{1.5.2}$$

The weak trilinear radiated field is superposed with a local oscillator $\mathbf{E}_D(t)$, and difference-detection determines the change in electromagnetic energy between $\mathbf{E}_D(t)+\mathbf{E}_{ABC}(t)$ and $\mathbf{E}_D(t)$ alone.[9] The *FWM signal* is therefore

$$\begin{aligned} \Delta\mathcal{U}(t) &= \frac{1}{4\pi}\int d^3R\,\left[\left(\mathbf{E}_D(t)+\mathbf{E}_{ABC}(t)\right)^2 - \mathbf{E}_D^2(t)\right] \\ &\cong \frac{1}{2\pi}\int d^3R\,\mathbf{E}_D(t)\cdot\mathbf{E}_{ABC}(t), \end{aligned} \tag{1.5.3}$$

where the integration volume—of approximate size $c\sigma_D\mathcal{A}$, where $\mathcal{A}$ is the cross-sectional area of the D-beam in the far-field region—contains the local oscillator light pulse at time t. The FWM signal does not depend on the precise value chosen for t, provided it is late enough that $\mathbf{E}_D(t)$ is localized a long distance from the sample volume. We let $t = (R_\circ/c) + t_D$, where $\mathbf{R}_\circ = R_\circ\mathbf{n}_D$ is a representative sample-to-field-point distance vector, write $\Delta\mathbf{R} = \mathbf{R} - \mathbf{R}_\circ$, and make the approximation $\mathbf{E}_D\cdot\mathbf{n} \cong \mathbf{E}_D\cdot\mathbf{n}_D$ to obtain

$$\Delta\mathcal{U} = \frac{\rho\Omega^2}{2\pi c^2 R_\circ}\int d^3(\Delta R)\int d^3r\,\mathbf{E}_D\left(t_D + \frac{R_\circ}{c}\right)\cdot\mathbf{m}_{ABC}\left(t_D - \frac{\mathbf{n}_D}{c}\cdot(\Delta\mathbf{R}-\mathbf{r})\right). \tag{1.5.4}$$

[8] See, for example, L. D. Landau and E. M. Lifshitz, *The Classical Theory of Fields*, 4th revised English edition (Pergamon Press, Oxford, 1975) Section 67.

[9] In applications of spectral interferometry to FWM, the superposed trilinear-signal and local-oscillator fields are filtered by frequency before their energy is measured (see Section 1.7).

Exercises:

- Justify the form given in Eq. (1.5.4) for the time-argument of the trilinear dipole moment.
- Would the FWM signal expression (1.5.4) change in any way if the local oscillator beam did pass through the sample?

To calculate $\mathbf{m}_{ABC}\left(t_D + (\mathbf{n}_D/c)\cdot(\mathbf{r}-\Delta\mathbf{R})\right)$, we need only determine the various nuclear amplitudes—wave packets—appearing in Eq. (1.4.10) on page 18. Rather than display formulas for all the required amplitudes, we show just a few and leave it as an exercise to write out the remainder. Although it is not necessary to do so under the present treatment, we henceforward make the additional simplifying assumption that *all four pulses are temporally nonoverlapping.* With appeal to Eq. (1.4.4) we find, for instance,

$$\left[t_{DA} + \mathbf{n}_{DA}\cdot\frac{\mathbf{r}}{c} - \mathbf{n}_D\cdot\frac{\Delta\mathbf{R}}{c}\right]_{00}|\psi_\circ\rangle \cong \left[t_{DA} - \mathbf{n}_D\cdot\frac{\Delta\mathbf{R}}{c}\right]_{00}|\psi_\circ\rangle\,; \tag{1.5.5}$$

note that $\mathbf{n}_D\cdot\Delta\mathbf{R}/c \sim \sigma_D$, unlike $\mathbf{n}_{DA}\cdot\mathbf{r}/c$, may be nonnegligible on the vibrational or EET timescale.

Representative of the one-pulse wave packets needed for the FWM signal is

$$\begin{aligned}\left\langle \xi \left| \Psi_A\left(t_D + \frac{\mathbf{n}_D}{c}\cdot(\mathbf{r}-\Delta\mathbf{R})\right)\right\rangle &= \langle\xi|\left[t_{DA} + \mathbf{n}_{DA}\cdot\frac{\mathbf{r}}{c} - \mathbf{n}_D\cdot\frac{\Delta\mathbf{R}}{c}\right]P_A\,|gg\rangle\,|\psi_\circ\rangle \\ &= \sum_{\xi_1}\left[t_{DA} + \mathbf{n}_{DA}\cdot\frac{\mathbf{r}}{c} - \mathbf{n}_D\cdot\frac{\Delta\mathbf{R}}{c}\right]_{\xi\xi_1}\langle\xi_1|\,P_A\,|gg\rangle\,|\psi_\circ\rangle \\ &\cong\; iE_Ae^{-i\varphi_A - i(\mathbf{k}_D-\mathbf{k}_A)\cdot\mathbf{r}}\sum_{\xi_1}(\xi_1 0)_A\left[t_{DA} - \mathbf{n}_D\cdot\frac{\Delta\mathbf{R}}{c}\right]_{\xi\xi_1} p_A^{(\xi_1 0)}\,|\psi_\circ\rangle\,. \end{aligned} \tag{1.5.6}$$

In the last line of this equation, we have taken advantage of the temporal isolation of the laser pulses, which allows us to push the upper limit of integration to infinity and drop the time arguments of a reduced pulse propagator, writing $p_I^{(\xi\bar{\xi})}(\infty;\tau) = p_I^{(\xi\bar{\xi})}$. The other one-pulse wave packets follow similarly.

One two-pulse wave packet—in the electronic ground state—takes the form

$$\begin{aligned}\left\langle 0 \left| \Psi_{BC}\left(t_D + \frac{\mathbf{n}_D}{c}\cdot(\mathbf{r}-\Delta\mathbf{R})\right)\right\rangle &= -E_BE_Ce^{-i\varphi_B + i\varphi_C + i(\mathbf{k}_B-\mathbf{k}_C)\cdot\mathbf{r}} \\ \times\sum_{\xi_2\,\xi_3}(0\xi_3)_C(\xi_2 0)_B\left[t_{DC} - \mathbf{n}_D\cdot\frac{\Delta\mathbf{R}}{c}\right]_{00} & p_C^{(0\xi_3)}\,[t_{CB}]_{\xi_3\xi_2}\,p_B^{(\xi_2 0)}\,[t_{BA}]_{00}\,|\psi_\circ\rangle\,. \end{aligned} \tag{1.5.7}$$

Two more two-pulse wave packets in the electronic ground state and two in the doubly-excited state have similar forms. Finally, the three-pulse wave packets in the singly-excited manifold are given by

$$\left\langle \xi \left| \Psi_{ABC}\left(t_D + \frac{\mathbf{n}_D}{c}\cdot(\mathbf{r}-\Delta\mathbf{R})\right)\right\rangle = -iE_AE_BE_Ce^{i\varphi_{BA}-i\varphi_C-i(\mathbf{k}_D-\mathbf{k}_C+\mathbf{k}_B-\mathbf{k}_A)\cdot\mathbf{r}}$$

$$\times \sum_{\xi_1\,\xi_2\,\xi_3} (\xi_3 0)_C (0\xi_2)_B (\xi_1 0)_A \left[t_{DC} - \mathbf{n}_D\cdot\frac{\Delta\mathbf{R}}{c}\right]_{\xi\xi_3} p_C^{(\xi_3 0)}\,[t_{CB}]_{00}\,p_B^{(0\xi_2)}\,[t_{BA}]_{\xi_2\xi_1}\,p_A^{(\xi_1 0)}\,|\psi_\circ\rangle\,. \tag{1.5.8}$$

Exercise: Write out the formulas for the additional one- and two-pulse amplitudes—analogous to Eqs. (1.5.6) and (1.5.7), respectively—that are required for the trilinear dipole moment.

We can now work out expressions for the various contributions to the trilinear dipole moment; we will drop some time arguments when these are clear from context. For instance, the first term in Eq. (1.4.10) is found by combining Eqs. (1.5.5) and (1.5.8), which gives

$$\langle\psi_\circ|\left[-t_{DA} - \frac{\mathbf{n}_D}{c}\cdot(\mathbf{r}-\Delta\mathbf{R})\right]_{00}\mathbf{m}_{0\xi}\,\langle\xi\,|\Psi_{ABC}\rangle = -iE_AE_BE_Ce^{i\varphi_{BA}-i\varphi_C-i(\mathbf{k}_D-\mathbf{k}_C+\mathbf{k}_B-\mathbf{k}_A)\cdot\mathbf{r}}$$

$$\times \sum_{\xi_1\,\xi_2\,\xi_3} (\xi_3 0)_C (0\xi_2)_B (\xi_1 0)_A \,\langle\psi_\circ|\left[-t_{DA} + \mathbf{n}_D\cdot\frac{\Delta\mathbf{R}}{c}\right]_{00}\mathbf{m}_{0\xi}$$

$$\times \left[t_{DC} - \mathbf{n}_D\cdot\frac{\Delta\mathbf{R}}{c}\right]_{\xi\xi_3} p_C^{(\xi_3 0)}\,[t_{CB}]_{00}\,p_B^{(0\xi_2)}\,[t_{BA}]_{\xi_2\xi_1}\,p_A^{(\xi_1 0)}\,|\psi_\circ\rangle\,. \tag{1.5.9}$$

The second term in the trilinear dipole moment is found, with the help of Eqs. (1.5.6) and (1.5.7), to be

$$\langle\Psi_{BC}|\,0\rangle\,\mathbf{m}_{0\xi}\,\langle\xi\,|\Psi_A\rangle = -iE_AE_BE_Ce^{i\varphi_{BA}-i\varphi_C-i(\mathbf{k}_D-\mathbf{k}_C+\mathbf{k}_B-\mathbf{k}_A)\cdot\mathbf{r}}$$

$$\times \sum_{\xi_1\,\xi_2\,\xi_3} (0\xi_3)_C (\xi_2 0)_B (\xi_1 0)_A \,\langle\psi_\circ|\,[-t_{BA}]_{00}\,p_B^{(0\xi_2)}\,[-t_{CB}]_{\xi_2\xi_3}\,p_C^{(\xi_3 0)}\left[-t_{DC} + \mathbf{n}_D\cdot\frac{\Delta\mathbf{R}}{c}\right]_{00}$$

$$\times\mathbf{m}_{0\xi}\left[t_{DA} - \mathbf{n}_D\cdot\frac{\Delta\mathbf{R}}{c}\right]_{\xi\xi_1} p_A^{(\xi_1 0)}\,|\psi_\circ\rangle\,; \tag{1.5.10}$$

we have used the properties $\left(p_B^{(\xi_2 0)}\right)^\dagger = p_B^{(0\xi_2)}$ and $\left(p_C^{(0\xi_3)}\right)^\dagger = p_C^{(\xi_2 0)}$.

Exercise: Find expressions for the four remaining contributions to the trilinear dipole moment.

Evaluation of the FWM signal $\Delta\mathcal{U}$ on page 19 involves integration over $\Delta\mathbf{R}$ (throughout the volume instantaneously occupied by the local-oscillator field $\mathbf{E}_D$) and integration over $\mathbf{r}$ (throughout the sample) of the six contributing terms[10] arising from Eq. (1.4.10). The first of these, arising from Eq. (1.5.9), involves the integral

$$\int d^3(\Delta R) \underbrace{\left[-t_{DA} + \mathbf{n}_D \cdot \frac{\Delta\mathbf{R}}{c}\right]_{00}}_{[-t_{DA}][\mathbf{n}_D\cdot\Delta\mathbf{R}/c]_{00}} \mathbf{E}_D\left(t_D + \frac{R_\circ}{c}\right) \cdot \mathbf{m}_{0\xi} \underbrace{\left[t_{DC} - \mathbf{n}_D \cdot \frac{\Delta\mathbf{R}}{c}\right]_{\xi\xi_3}}_{\cong[-\mathbf{n}_D\cdot\Delta\mathbf{R}/c]_{\xi\xi}[t_{DC}]_{\xi\xi_3}}$$

$$= E_D(0\xi)_D\,[-t_{DA}]_{00} \int d^3(\Delta R) \left[\mathbf{n}_D \cdot \frac{\Delta\mathbf{R}}{c}\right]_{00} \left[-\mathbf{n}_D \cdot \frac{\Delta\mathbf{R}}{c}\right]_{\xi\xi}$$

$$\times \underbrace{f_D\Big(t_D + \frac{R_\circ}{c} - t_D(\mathbf{R})\Big)}_{f_D(-\mathbf{n}_D\cdot\Delta\mathbf{R}/c)} \cos\Big\{\Omega_D \underbrace{\Big(t_D + \frac{R_\circ}{c} - t_D(\mathbf{R})\Big)}_{-\mathbf{n}_D\cdot\Delta\mathbf{R}/c} + \varphi_D\Big\}\,[t_{DC}]_{\xi\xi_3}\,. \qquad (1.5.11)$$

Exercise: Justify the equality and approximate equality stated beneath the first line of Eq. (1.5.11).

With a variable change to $\tau = -\mathbf{n}_D \cdot \Delta\mathbf{R}/c$, we can write $\int d^3(\Delta R) \cdots \cong \mathcal{A}c \int d\tau \cdots$ (see page 19). Hence

$$\int d^3(\Delta R) \left[-t_{DA} + \mathbf{n}_D \cdot \frac{\Delta\mathbf{R}}{c}\right]_{00} \mathbf{E}_D\left(t_D + \frac{R_\circ}{c}\right) \cdot \mathbf{m}_{0\xi} \left[t_{DC} - \mathbf{n}_D \cdot \frac{\Delta\mathbf{R}}{c}\right]_{\xi\xi_3}$$

$$\cong \mathcal{A}cE_D(0\xi)_D\,[-t_{DA}]_{00} \int d\tau\,[-\tau]_{00}\,[\tau]_{\xi\xi}\,f_D\,(\tau) \cos\Big\{\Omega_D\tau + \varphi_D\Big\}\,[t_{DC}]_{\xi\xi_3}$$

$$\cong \mathcal{A}cE_D(0\xi)_D\,[-t_{DA}]_{00} \int d\tau\,[-\tau]_{00}\,[\tau]_{\xi\xi}\,f_D\,(\tau)\,\frac{1}{2}e^{i\Omega_D\tau + i\varphi_D}\,[t_{DC}]_{\xi\xi_3}$$

$$= \hbar\mathcal{A}cE_D(0\xi)_D e^{i\varphi_D}\,[-t_{DA}]_{00}\,p_D^{(0\xi)}\,[t_{DC}]_{\xi\xi_3}\,, \qquad (1.5.12)$$

where a rotating wave approximation has been made (third line) and a reduced pulse propagator has been introduced (fourth line; see page 15).

[10] Twelve terms, actually, when we account for the sum over two values of ξ.

Integration over the sample volume in the contribution to $\Delta\mathcal{U}$ arising from Eq. (1.5.9) involves an integral,

$$\int_V d^3r\, e^{-i(\mathbf{k}_D-\mathbf{k}_C+\mathbf{k}_B-\mathbf{k}_A)\cdot\mathbf{r}} \equiv \delta_V(\mathbf{k}_D-\mathbf{k}_C+\mathbf{k}_B-\mathbf{k}_A), \tag{1.5.13}$$

which becomes a three-dimensional, sharply peaked delta-like function that enforces a *wave-vector matching condition* $\mathbf{k}_D \cong \mathbf{k}_C-\mathbf{k}_B+\mathbf{k}_A$ between the incident and the local-oscillator wave vectors.[11]

Repeated use of relations analogous to Eqs. (1.5.12) and (1.5.13), and the simplifying omission of free molecular-evolution operators—all for interpulse delays reckoned at the sample origin—that appear between the reduced pulse propagators in the various wave-packet overlaps, lead to a final expression for the FWM signal, $\Delta\mathcal{U}=\Delta\mathcal{U}_{reph}+\Delta\mathcal{U}_{non}$. The *rephasing signal* is

$$\begin{aligned}
\Delta\mathcal{U}_{reph} &= E_AE_BE_CE_D\frac{\hbar\rho\mathcal{A}\Omega^2}{\pi cR_\circ}\mathrm{Im}\sum_{\xi_1\xi_2\xi_3\xi_4} e^{i\varphi_{BA}-i\varphi_{DC}}\delta_V(\mathbf{k}_{BA}-\mathbf{k}_{DC})\\
&\quad\times\Big\{-(\xi_40)_D(0\xi_3)_C(\xi_20)_B(\xi_10)_A\,\langle\psi_\circ|\,p_B^{(0\xi_2)}p_D^{(\xi_40)}p_C^{(0\xi_3)}p_A^{(\xi_10)}\,|\psi_\circ\rangle\\
&\quad-(\xi_40)_D(\xi_30)_C(0\xi_2)_B(\xi_10)_A\,\langle\psi_\circ|\,p_C^{(0\xi_3)}p_D^{(\xi_40)}p_B^{(0\xi_2)}p_A^{(\xi_10)}\,|\psi_\circ\rangle\\
&\quad+(2\xi_4)_D(2\xi_3)_C(\xi_20)_B(\xi_10)_A\,\langle\psi_\circ|\,p_B^{(0\xi_2)}p_C^{(\xi_32)}p_D^{(2\xi_4)}p_A^{(\xi_10)}\,|\psi_\circ\rangle\Big\},
\end{aligned} \tag{1.5.14}$$

and the *nonrephasing signal* is

$$\begin{aligned}
\Delta\mathcal{U}_{non} &= E_AE_BE_CE_D\frac{\hbar\rho\mathcal{A}\Omega^2}{\pi cR_\circ}\mathrm{Im}\sum_{\xi_1\xi_2\xi_3\xi_4} e^{i\varphi_{BA}+i\varphi_{DC}}\delta_V(\mathbf{k}_{BA}+\mathbf{k}_{DC})\\
&\quad\times\Big\{(0\xi_4)_D(\xi_30)_C(0\xi_2)_B(\xi_10)_A\,\langle\psi_\circ|\,p_D^{(0\xi_4)}p_C^{(\xi_30)}p_B^{(0\xi_2)}p_A^{(\xi_10)}\,|\psi_\circ\rangle\\
&\quad+(0\xi_4)_D(0\xi_3)_C(\xi_20)_B(\xi_10)_A\,\langle\psi_\circ|\,p_B^{(0\xi_2)}p_C^{(\xi_30)}p_D^{(0\xi_4)}p_A^{(\xi_10)}\,|\psi_\circ\rangle\\
&\quad-(\xi_42)_D(2\xi_3)_C(\xi_20)_B(\xi_10)_A\,\langle\psi_\circ|\,p_B^{(0\xi_2)}p_D^{(\xi_42)}p_C^{(2\xi_3)}p_A^{(\xi_10)}\,|\psi_\circ\rangle\Big\}.
\end{aligned} \tag{1.5.15}$$

The rephasing and nonrephasing signals appear in different phase-matched directions and carry concomitantly different optical phase signatures.

Exercise: Provide physical justification for the terminology introduced to identify Eqs. (1.5.14) and (1.5.15).

[11] Note that $\delta_V(\mathbf{0})=V$.

In the derivation of $\Delta\mathcal{U}$ (and the md-WPI signal below), all the transition dipole orientations are regarded as fixed and uniform relative to the linear laser polarizations. To find the signals for an isotropic sample in which molecular orientations are, moreover, uncorrelated with position, we simply replace the four-fold products of transition-dipole projections by the corresponding angularly averaged quantities, such as

$$(0\xi_4)_D(\xi_3 0)_C(0\xi_2)_B(\xi_1 0)_A \rightarrow \big\langle (0\xi_4)_D(\xi_3 0)_C(0\xi_2)_B(\xi_1 0)_A \big\rangle, \tag{1.5.16}$$

and make use of standard expressions for these orientationally averaged products.

1.6 Wave-packet interferometry signal

A fluorescence-detected md-WPI measurement determines the action signal

$$\begin{aligned} S &= \rho \int_V d^3r \big\{ Q_2 S^{(2)} + Q_1 S^{(1)} + Q_{1'} S^{(1')} \big\} \\ &= \rho \int_V d^3r \big\{ Q_{ee} S^{(ee)} + Q_{eg} S^{(eg)} + Q_{ge} S^{(ge)} \big\}, \end{aligned} \tag{1.6.1}$$

in which the various quadrilinear electronic-state populations S_ξ are those formally determined at the local D-pulse arrival time $t_D + \mathbf{n_D}\cdot\mathbf{r}/c$ (see Eqs. (1.4.11) and (1.4.12)) and the Q_ξ are level-specific fluorescence quantum yields.

We need bilinear nuclear wave packets in the two-exciton state, such as

$$\begin{aligned} \big\langle 2\big|\Psi_{AD}\big\rangle &= -E_A E_D e^{-i\varphi_A - i\varphi_D + i(\mathbf{k}_A - \mathbf{k}_D)\cdot\mathbf{r}} \\ &\quad \times \sum_{\xi_1\xi_4} (2\xi_4)_D(\xi_1 0)_A p_D^{(2\xi_4)} \, [t_{DA}]_{\xi_4\xi_1} \, p_A^{(\xi_1 0)} \, |\psi_\circ\rangle \end{aligned} \tag{1.6.2}$$

and

$$\begin{aligned} \big\langle 2\big|\Psi_{BC}\big\rangle &= -E_B E_C e^{-i\varphi_B - i\varphi_C + i(\mathbf{k}_B + \mathbf{k}_C - 2\mathbf{k}_D)\cdot\mathbf{r}} \\ &\quad \times \sum_{\xi_2\xi_3} (2\xi_3)_C(\xi_2 0)_B \, [t_{DC}]_{22} \, p_C^{(2\xi_3)} \, [t_{CB}]_{\xi_3\xi_2} \, p_B^{(\xi_2 0)} \, [t_{BA}]_{00} \, |\psi_\circ\rangle \, . \end{aligned} \tag{1.6.3}$$

Eqs. (1.6.2) and (1.6.3), along with the additional bilinear, two-exciton amplitudes $\big\langle 2\big|\Psi_{AC}\big\rangle$ and $\big\langle 2\big|\Psi_{BD}\big\rangle$, lead to the quadrilinear population of the two-exciton state,

$$\begin{aligned} S^{(ee)} &= S^{(2)} = E_A E_B E_C E_D 2\mathrm{Re} \sum_{\xi_1\xi_2\xi_3\xi_4} (2\xi_4)_D(2\xi_3)_C(\xi_2 0)_B(\xi_1 0)_A \\ &\quad \times \Big\{ e^{i\varphi_{BA} - i\varphi_{DC} - i(\mathbf{k}_{BA} - \mathbf{k}_{DC})\cdot\mathbf{r}} \, \langle\psi_\circ| \, p_B^{(0\xi_2)} p_C^{(\xi_3 2)} p_D^{(2\xi_4)} p_A^{(\xi_1 0)} \, |\psi_\circ\rangle \\ &\quad + e^{i\varphi_{BA} + i\varphi_{DC} - i(\mathbf{k}_{BA} + \mathbf{k}_{DC})\cdot\mathbf{r}} \, \langle\psi_\circ| \, p_B^{(0\xi_2)} p_D^{(\xi_4 2)} p_C^{(2\xi_3)} p_A^{(\xi_1 0)} \, |\psi_\circ\rangle \Big\}; \end{aligned} \tag{1.6.4}$$

interpulse free-evolution operators are again omitted.

Exercise: Find expressions for $\langle 2|\Psi_{AC}\rangle$ and $\langle 2|\Psi_{BD}\rangle$, and verify formula (1.6.4) for the quadrilinear two-exciton population.

We also need four one-pulse and four three-pulse wave packets in the one-exciton manifold, like

$$\langle \xi_4|\Psi_A\rangle = iE_A e^{-i\varphi_A+i(\mathbf{k}_A-\mathbf{k}_D)\cdot\mathbf{r}} \sum_{\xi_1} (\xi_1 0)_A \, [t_{DA}]_{\xi_4\xi_1} \, p_A^{(\xi_1 0)} \, |\psi_\circ\rangle \tag{1.6.5}$$

and

$$\begin{aligned}
\langle \xi_4|\Psi_{BCD}\rangle \;=\; & -iE_B E_C E_D e^{-i\varphi_B+i\varphi_{DC}+i(\mathbf{k}_B-2\mathbf{k}_D+\mathbf{k}_C)\cdot\mathbf{r}} \sum_{\xi_2\xi_3} (\xi_4 2)_D (2\xi_3)_C (\xi_2 0)_B \\
& \times p_D^{(\xi_4 2)} \, [t_{DC}]_{22} \, p_C^{(2\xi_3)} \, [t_{CB}]_{\xi_3\xi_2} \, p_B^{(\xi_2 0)} \, [t_{BA}]_{00} \, |\psi_\circ\rangle \\
& -iE_B E_C E_D e^{-i\varphi_B-i\varphi_{DC}+i(\mathbf{k}_B-\mathbf{k}_C)\cdot\mathbf{r}} \sum_{\xi_2\xi_3} (\xi_4 0)_D (0\xi_3)_C (\xi_2 0)_B \\
& \times p_D^{(\xi_4 0)} \, [t_{DC}]_{00} \, p_C^{(0\xi_3)} \, [t_{CB}]_{\xi_3\xi_2} \, p_B^{(\xi_2 0)} \, [t_{BA}]_{00} \, |\psi_\circ\rangle \, ,
\end{aligned} \tag{1.6.6}$$

respectively. From these, we obtain the quadrilinear population of the one-exciton states,

$$\begin{aligned}
S^{(\xi_4)} \;=\; & -E_A E_B E_C E_D 2\mathrm{Re} \sum_{\xi_1\xi_2\xi_3} e^{i\varphi_{BA}-i\varphi_{DC}-i(\mathbf{k}_{BA}-\mathbf{k}_{DC})\cdot\mathbf{r}} \\
& \times \Big\{ (\xi_4 0)_D (\xi_3 0)_C (0\xi_2)_B (\xi_1 0)_A \, \langle\psi_\circ| \, p_C^{(0\xi_3)} p_D^{(\xi_4 0)} p_B^{(0\xi_2)} p_A^{(\xi_1 0)} \, |\psi_\circ\rangle \\
& + (\xi_4 0)_D (0\xi_3)_C (\xi_2 0)_B (\xi_1 0)_A \, \langle\psi_\circ| \, p_B^{(0\xi_2)} p_D^{(\xi_4 0)} p_C^{(0\xi_3)} p_A^{(\xi_1 0)} \, |\psi_\circ\rangle \\
& + (\xi_4 2)_D (2\xi_3)_C (\xi_2 0)_B (\xi_1 0)_A \, \langle\psi_\circ| \, p_B^{(0\xi_2)} p_C^{(\xi_3 2)} p_D^{(2\xi_4)} p_A^{(\xi_1 0)} \, |\psi_\circ\rangle \Big\} \\
& - E_A E_B E_C E_D 2\mathrm{Re} \sum_{\xi_1\xi_2\xi_3} e^{i\varphi_{BA}+i\varphi_{DC}-i(\mathbf{k}_{BA}+\mathbf{k}_{DC})\cdot\mathbf{r}} \\
& \times \Big\{ (\xi_4 0)_D (\xi_3 0)_C (0\xi_2)_B (\xi_1 0)_A \, \langle\psi_\circ| \, p_D^{(0\xi_4)} p_C^{(\xi_3 0)} p_B^{(0\xi_2)} p_A^{(\xi_1 0)} \, |\psi_\circ\rangle \\
& + (\xi_4 0)_D (0\xi_3)_C (\xi_2 0)_B (\xi_1 0)_A \, \langle\psi_\circ| \, p_B^{(0\xi_2)} p_C^{(\xi_3 0)} p_D^{(0\xi_4)} p_A^{(\xi_1 0)} \, |\psi_\circ\rangle \\
& + (\xi_4 2)_D (2\xi_3)_C (\xi_2 0)_B (\xi_1 0)_A \, \langle\psi_\circ| \, p_B^{(0\xi_2)} p_D^{(\xi_4 2)} p_C^{(2\xi_3)} p_A^{(\xi_1 0)} \, |\psi_\circ\rangle \Big\}.
\end{aligned} \tag{1.6.7}$$

Exercise: Work out the expressions for the additional one-exciton wave packets, $\langle \xi_4 | \Psi_B \rangle$, $\langle \xi_4 | \Psi_C \rangle$, $\langle \xi_4 | \Psi_D \rangle$, $\langle \xi_4 | \Psi_{ACD} \rangle$, $\langle \xi_4 | \Psi_{ABD} \rangle$, and $\langle \xi_4 | \Psi_{ABC} \rangle$, and complete the derivation of Eq. (1.6.7) for the quadrilinear single-exciton population.

Multidimensional wave-packet interferometry measurements carry the advantage that, where applicable, they can be performed on a single molecule (in the case of interest here, on a single energy-transfer complex). In contrast, four-wave mixing requires the generation of a directional signal beam emanating from a spatially extended sample containing many chromophores. In a single-molecule md-WPI experiment, the signal—averaged over many repetitions, with the EET complex in a fixed position and orientation—would be simply

$$S = Q_2 S^{(2)} + \sum_{\xi = 1'1 \,(\text{or } ge\, eg)} Q_\xi S^{(\xi)}, \tag{1.6.8}$$

which can be calculated using the formulas (1.6.4) and (1.6.7).

When md-WPI is applied to the same extended sample whose FWM signals are given by Eqs. (1.5.14) and (1.5.15), the signal (1.6.1) takes the form $S = S_{reph} + S_{non}$, where

$$\begin{aligned} S_{reph} \;=\; & E_A E_B E_C E_D 2\rho \mathrm{Re} \sum_{\xi_1\xi_2\xi_3\xi_4} e^{i\varphi_{BA} - i\varphi_{DC}} \delta_V(\mathbf{k}_{BA} - \mathbf{k}_{DC}) \\ & \times \Big\{ \Big(Q_2 - Q_{\xi_4} \Big) (2\xi_4)_D (2\xi_3)_C (\xi_2 0)_B (\xi_1 0)_A \, \langle \psi_\circ | \, p_B^{(0\xi_2)} p_C^{(\xi_3 2)} p_D^{(2\xi_4)} p_A^{(\xi_1 0)} \, | \psi_\circ \rangle \\ & - Q_{\xi_4} (\xi_4 0)_D (\xi_3 0)_C (\xi_2 0)_B (\xi_1 0)_A \Big(\langle \psi_\circ | \, p_C^{(0\xi_3)} p_D^{(\xi_4 0)} p_B^{(0\xi_2)} p_A^{(\xi_1 0)} \, | \psi_\circ \rangle \\ & + \langle \psi_\circ | \, p_B^{(0\xi_2)} p_D^{(\xi_4 0)} p_C^{(0\xi_3)} p_A^{(\xi_1 0)} \, | \psi_\circ \rangle \Big) \Big\} \end{aligned} \tag{1.6.9}$$

and

$$\begin{aligned} S_{non} \;=\; & E_A E_B E_C E_D 2\rho \mathrm{Re} \sum_{\xi_1\xi_2\xi_3\xi_4} e^{i\varphi_{BA} + i\varphi_{DC}} \delta_V(\mathbf{k}_{BA} + \mathbf{k}_{DC}) \\ & \times \Big\{ \Big(Q_2 - Q_{\xi_4} \Big) (2\xi_4)_D (2\xi_3)_C (\xi_2 0)_B (\xi_1 0)_A \, \langle \psi_\circ | \, p_B^{(0\xi_2)} p_D^{(\xi_4 2)} p_C^{(2\xi_3)} p_A^{(\xi_1 0)} \, | \psi_\circ \rangle \\ & - Q_{\xi_4} (\xi_4 0)_D (\xi_3 0)_C (\xi_2 0)_B (\xi_1 0)_A \Big(\langle \psi_\circ | \, p_D^{(0\xi_4)} p_C^{(\xi_3 0)} p_B^{(0\xi_2)} p_A^{(\xi_1 0)} \, | \psi_\circ \rangle \\ & + \langle \psi_\circ | \, p_B^{(0\xi_2)} p_C^{(\xi_3 0)} p_D^{(0\xi_4)} p_A^{(\xi_1 0)} \, | \psi_\circ \rangle \Big) \Big\}. \end{aligned} \tag{1.6.10}$$

If $Q_2 = 2$ and both $Q_\xi = 1$, then the time- and frequency-integrated fluorescence gives a count of stored photons; every absorbed photon leads to a fluorescence photon, and the linear absorption spectrum of the complex coincides with the fluorescence excitation spectrum. In this situation, we should expect that the $\Delta \mathcal{U} \propto \hbar \Omega S$, and the FWM signal of a given wave vector-matched direction should be proportional to the md-WPI of the corresponding optical phase signature. Comparison of Eq. (1.5.14) with Eq. (1.6.9), and Eq. (1.5.15) with (1.6.10), shows that this proportionality does obtain when $Q_2 : Q_\xi$

is 2:1.[12] Departures of the two-photon to one-photon quantum yields from two-to-one proportionality can lead to differences in dynamical information content between FWM and md-WPI signals.

Exercise: If the local-oscillator beam passes through the sample, rather than bypassing it, then corresponding FWM signals and md-WPI signals (times $\hbar\Omega$) should be essentially *equal* in the case where $Q_2 = 2$ and $Q_\xi = 1$. Show that this is so by verifying the equality of $E_D(ff)\hbar\rho\mathcal{A}\Omega^2/(\pi c R_\circ)$ and $\hbar\Omega E_D(samp)2\rho$; use the fact that the local-oscillator field strengths in the far field and at the sample are related by $E_D^2(ff)\eta R_\circ^2 = E_D^2(samp)\pi(d/2)^2$, where $\eta = \pi\delta\theta^2/4$ is the solid angle of the beams emanating from the sample-spot, along with the estimate $\delta\theta = 4\lambda/(\pi d)$.

1.7 FWM by spectral interferometry

The technique of *spectral interferometry* typically sends the local-oscillator pulse through the sample ahead of the A, B, and C pulses ($t_D < t_A \leq t_B \leq t_C$) and filters the superposed signal and local-oscillator fields by frequency before detection. After spectral filtering at frequency $\bar\omega$ with a slit-width $\delta\omega$, a time-dependent field with Fourier components $\tilde E(\omega) = \int_{-\infty}^{\infty} dt\, e^{i\omega t}E(t)$ becomes

$$\begin{aligned} E'(t;\bar\omega) &= \int_{\bar\omega-\frac{\delta\omega}{2}}^{\bar\omega+\frac{\delta\omega}{2}} \frac{d\omega}{2\pi}\, e^{-i\omega t}\tilde E(\omega) + \int_{-\bar\omega-\frac{\delta\omega}{2}}^{-\bar\omega+\frac{\delta\omega}{2}} \frac{d\omega}{2\pi}\, e^{-i\omega t}\tilde E(\omega) \\ &= 2\mathrm{Re}\int_{\bar\omega-\frac{\delta\omega}{2}}^{\bar\omega+\frac{\delta\omega}{2}} \frac{d\omega}{2\pi}\, e^{-i\omega t}\tilde E(\omega) \\ &= 2\int_{-\infty}^{\infty} dt'\, \cos\bar\omega(t-t')\,\frac{\sin\frac{\delta\omega}{2}(t-t')}{\pi(t-t')}\,E(t')\,. \end{aligned} \tag{1.7.1}$$

Since $(\pi(t-t'))^{-1}\sin\frac{\delta\omega}{2}(t-t')$ is peaked at $t=t'$ and falls to zero at $t = t' \pm 2\pi/\delta\omega$, the filtration greatly elongates a pulse $E(t)$ with duration $\sigma << 2\pi/\delta\omega$.

---

[12] Phase differences of $\pi/2$ between contributions to $\Delta\mathcal{U}$ and S of the same phase signature can be attributed to the lag of a quarter-cycle in coherent emission; these phase shifts correspond to time delays of $\pi/(2\Omega)$, which are irrelevant on the timescales of EET and vibrational dynamics.

Exercise: Find a compact form for the spectrally filtered local-oscillator pulse $\mathbf{E}'_D(t;\bar{\omega})$ given by Eq. (1.2.4).

The change in electromagnetic energy due to the interference between two co-propagating filtered fields $E'(t;\bar{\omega})$ and $F'(t;\bar{\omega})$ is

$$\begin{aligned}\frac{1}{2\pi}\int d^3R\, E'(t;\bar{\omega})F'(t;\bar{\omega}) &= \frac{1}{2\pi}\int d^3R\Big(\int\limits_{\bar{\omega}-\frac{\delta\omega}{2}}^{\bar{\omega}+\frac{\delta\omega}{2}}\frac{d\omega}{2\pi}\,e^{-i\omega t}\tilde{E}(\omega,\mathbf{R})+c.c.\Big)\\ &\quad\times\Big(\int\limits_{\bar{\omega}-\frac{\delta\omega}{2}}^{\bar{\omega}+\frac{\delta\omega}{2}}\frac{d\omega'}{2\pi}\,e^{-i\omega' t}\tilde{F}(\omega',\mathbf{R})+c.c.\Big).\end{aligned}\tag{1.7.2}$$

Substituting $\tilde{E}(\omega,\mathbf{R}) = e^{i\omega\mathbf{n}\cdot\Delta\mathbf{R}/c}\tilde{E}(\omega,\mathbf{R}_\circ)$ and $\tilde{F}(\omega',\mathbf{R}) = e^{i\omega'\mathbf{n}\cdot\Delta\mathbf{R}/c}\tilde{F}(\omega',\mathbf{R}_\circ)$, where $\mathbf{R} = \mathbf{R}_\circ + \Delta\mathbf{R}$, and assuming a common beam area $\mathcal{A}$ gives

$$\frac{1}{2\pi}\int d^3R\, E'(t;\bar{\omega})F'(t;\bar{\omega}) = \frac{\mathcal{A}c}{\pi}\mathrm{Re}\int\limits_{\bar{\omega}-\frac{\delta\omega}{2}}^{\bar{\omega}+\frac{\delta\omega}{2}}\frac{d\omega}{2\pi}\,\tilde{E}^*(\omega,\mathbf{R}_\circ)\tilde{F}(\omega,\mathbf{R}_\circ)\,.\tag{1.7.3}$$

Because it is enough that the Fourier components of *either* field be restricted to the selected range, we would get the same expression for the interference between $E'(t;\bar{\omega})$ and $F(t)$ (or $E(t)$ and $F'(t;\bar{\omega})$). In evaluating the spectrally resolved FWM signal, we may therefore use

$$\Delta\mathcal{U}'(\bar{\omega}) = \frac{1}{2\pi}\int d^3R\,\mathbf{E}'_D(t;\bar{\omega})\cdot\mathbf{E}_{ABC}(t)\,,\tag{1.7.4}$$

where the time is late enough that both the signal and the filtered local-oscillator field lie in the far-field region. To be definite, we take $t = t_D + R_\circ/c$, and sketch in Fig. (1.7.1) the spatial distribution of the fields leading to $\Delta\mathcal{U}'(\bar{\omega})$.

Writing $\mathbf{E}'_D(t_D+R_\circ/c;\bar{\omega})$ similarly to Eq. (1.7.1) and changing the integration variable to $\tau = t_D + (R_\circ/c) - t'$ gives the spectrally-resolved FWM signal in the suggestive form

$$\Delta\mathcal{U}'(\bar{\omega}) = 2\int\limits_{-\infty}^{\infty}d\tau\,\cos\bar{\omega}\tau\,\frac{\sin\frac{\delta\omega}{2}\tau}{\pi\tau}\,\underbrace{\frac{1}{2\pi}\int d^3R\,\mathbf{E}_D(t_D+\frac{R_\circ}{c}-\tau)\cdot\mathbf{E}_{ABC}(t_D+\frac{R_\circ}{c})}\,.\tag{1.7.5}$$

The under-bracketed quantity is the spectrally *unresolved* FWM signal with the D pulse delayed by τ from its actual arrival time. Because the unresolved signal vanishes when the local oscillator precedes the advent of the trilinear signal field, we could, with neglect of pulse-ovelap effects, replace the lower limit of the τ-integration by t_{CD}. From the

Figure 1.7.1: E'_D represents the spectrally filtered—hence temporally and spatially stretched—local-oscillator pulse, whose interference with the FWM signal field E_{ABC} gives rise to the spectral interferogram $\Delta\mathcal{U}'(\bar{\omega})$.

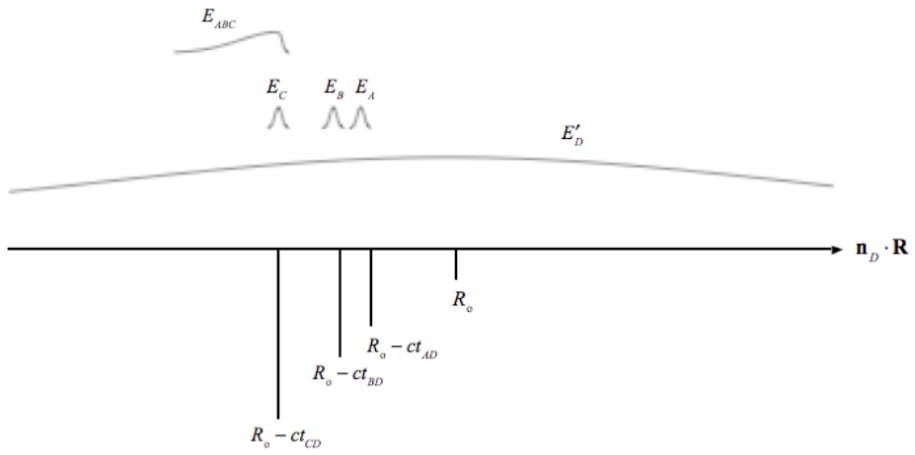

spectral interferogram—consisting of $\Delta\mathcal{U}'(\bar{\omega})$ for all frequencies yielding nonnegligible signal—it is readily possible to reconstruct the full time-dependent interferogram. Using $\int_{-\infty}^{\infty}(d\bar{\omega}/2\pi)\,\exp(-i\bar{\omega}t)\,\cos(\bar{\omega}\tau) = (1/2)\delta(t-\tau)$, for positive t, we find

$$\begin{aligned}\frac{\sin\frac{\delta\omega}{2}t}{\pi t}\,\Delta\mathcal{U}_{t_D\to t_D+t} &= \frac{\sin\frac{\delta\omega}{2}t}{2\pi^2 t}\int d^3R\,\mathbf{E}_D(t_D+\frac{R_\circ}{c}-t)\cdot\mathbf{E}_{ABC}(t_D+\frac{R_\circ}{c}) \\ &= \int_{-\infty}^{\infty}\frac{d\bar{\omega}}{2\pi}\,e^{-i\bar{\omega}t}\Delta\mathcal{U}'(\bar{\omega})\,. \qquad (1.7.6)\end{aligned}$$

1.8 Illustrative measured and calculated signals

*****

1.9 End-of-chapter problems

1. FT of DeltaU-prime wrt to t_BA; the 2D frequency-frequency interferogram. For negative t_BA must use DeltaU-prime with opposite phase matching condition.

2. Phase-modulation for 2D electronic coherence spectroscopy.

3. Reconstruction of E_ABC from t_D-scanned FWM or md-WPI data or from spectral interferogram.

4. The fluorescence-detected pump-probe limit of md-WPI, including A-B & C-D pulse-overlap effects.

1.10 Bibliography